Tracking far-range air pollution induced by the 2014–15 Bárdarbunga fissure eruption (Iceland)

Marie Boichu[1], Isabelle Chiapello[1], Colette Brogniez[1], Jean-Christophe Péré[1], Francois Thieuleux[1], Benjamin Torres[1], Luc Blarel[1], Augustin Mortier[2], Thierry Podvin[1], Philippe Goloub[1], Nathalie Söhne[3], Lieven Clarisse[4], Sophie Bauduin[4], François Hendrick[5], Nicolas Theys[5], Michel Van Roozendael[5], and Didier Tanré[1]

[1]Laboratoire d'Optique Atmosphérique, Université Lille 1, CNRS/INSU, UMR8518, Villeneuve d'Ascq, France
[2]Norwegian Meteorological Institute, Oslo, Norway
[3]Atmo Nord–Pas-De-Calais, Lille, France
[4]Spectroscopie de l'Atmosphère, Service de Chimie Quantique et Photophysique, Université Libre de Bruxelles, Brussels, Belgium
[5]Belgian Institute for Space Aeronomy (BIRA-IASB), Brussels, Belgium

Correspondence to: Marie Boichu, marie.boichu@univ-lille1.fr

Abstract. The 2014–15 Holuhraun lava-flood eruption of Bárdarbunga volcano (Iceland) has emitted prodigious amounts of sulfur dioxide into the atmosphere. This eruption caused a large-scale episode of air pollution throughout Western Europe in September 2014, the first event of this magnitude recorded in the modern era. We gathered a wealth of complementary observations from satellite sensors (OMI, IASI), ground-based remote sensing (lidar, sunphotometry, differential optical absorption spectroscopy) and ground-level air quality monitoring networks to characterize both the spatial-temporal distributions of volcanic SO_2 and sulfate aerosols as well as the dynamics of the planetary boundary layer. Time variations of dynamical and microphysical properties of sulfate aerosols in the aged low-tropospheric volcanic cloud, including loading, vertical distribution, size distribution and single scattering albedo, are provided. Retrospective chemistry-transport simulations capture the correct temporal dynamics of this far-range air pollution event but fail to reproduce the magnitude of SO_2 concentration at ground-level. Improving forecasts of large-scale volcanogenic air pollution will require refined emission parameters and adapted model grid resolution to accurately describe both long-range transport and local boundary layer dynamics.

1 Introduction

On a local scale, the detrimental impact of volcanic gas, acid aerosol and ash emissions on the atmospheric environment (air pollution, rain acidification) and terrestrial ecosystems (soil, vegetation, groundwater, animals and humans) is well recognized (Delmelle, 2003; Hansell and Oppenheimer, 2004; Longo et al., 2008; van Manen, 2014; Horwell and Baxter, 2006; Ayris and Delmelle, 2012). However, volcanic sulphur-rich degassing can also generate air pollution events on a continental scale. Historical archives record evidences of long-range transport of acidic gases and aerosols from the 1783–84 Laki lava flood eruption (Iceland) up to Western and Central Europe (Thordarson and Self, 2003). Concomitantly, an abnormally high human mortality rate was observed not only in Iceland but also in Western Europe (Thordarson and Self, 2003; Witham and Oppenheimer, 2004;

20   Grattan et al., 2005; Oppenheimer, 2011). In the specific case of the Laki eruption, it is difficult to draw a distinction between the respective impacts of volcanogenic air pollution and severe meteorological conditions, as extremes of heat and cold (which may have been partly caused by the eruption itself) occurred concurrently with the eruption (Oppenheimer, 2011). Neverthe-less, there is little doubt that a Laki-style eruption would cause severe health hazards leading to an excess mortality rate at a continental scale (Schmidt et al., 2011). Obviously, at the time of the Laki eruption, only sparse observations on meteorological

25   conditions (Yiou et al., 2014) and dispersed volcanic compounds (Thordarson and Self, 2003) were available, which hinders a thorough test of our ability to accurately model the dispersal of the prodigious emissions of volcanic SO_2 toward remote regions.

The long-lasting Holuhraun lava flood eruption (Aug 2014–Feb 2015) within the Bárdarbunga volcanic system (Iceland), hereafter called "Bárdarbunga eruption", allows for quantitatively assessing the far-range impact of a volcanic eruption on air quality. Even if of lesser magnitude than Laki (about one order of magnitude smaller in terms of emitted lava and sulphur

5   degassing budgets (Gíslason et al., 2015)), the 6 month-long Bárdarbunga eruption continuously emitted abundant quantities of SO_2 into the lower troposphere reaching 11–12 Mt according to petrological estimates and ground-based UV-DOAS (Dif-ferential Optical Absorption Spectroscopy) observations (Gíslason et al., 2015). Whereas SO_2 air pollution is generally of anthropogenic origin, mainly associated with the combustion of sulfur-rich fossil fuels or with mining activities, the Bárdar-bunga emissions have exceeded the budget of SO_2 emitted annually by all 28 state members of the European Union (4.6 Mt

10   in 2011 (European Environment Agency, 2014)). Even so, the Bárdarbunga eruption only weakly disturbed air traffic manage-ment compared to 2010 Eyjafjallajökull and 2011 Grimsvötn ash-rich icelandic eruptions. Nevertheless, Bárdarbunga volcano triggered a volcanogenic air pollution unprecedented in Europe in the modern era, which necessitated locally exceptional civil protection measures (Gíslason et al., 2015). Indeed, high ground-level concentration of SO_2 and sulfate aerosols, mainly issued from the conversion of SO_2 in the atmosphere, is harmful to human health. SO_2 concentrations up to 9000–21000 μg.m^{-3} were

15   recorded in Iceland at a hundred kilometers from the eruption site, i.e. $\sim$60 times the hourly exposure limit value of 350 μg.m^{-3} fixed by World Health Organization (WHO) (Gíslason et al., 2015).

The Bárdarbunga cloud travelled most often from the eruption site toward high latitudes, beyond the Arctic Polar Circle. However, owing to peculiar meteorological conditions, the volcanic cloud was transported toward Western Europe in Septem-ber 2014. This event fueled a far-range pollution event in SO_2 and particles which was recorded, without being exhaustive, in

20   Fenno-Scandinavia (Ialongo et al., 2015; Grahn et al., 2015), Ireland, UK, the Netherlands (Schmidt et al., 2015) and France (Boichu, 2015). Contrary to stratospheric sulfate aerosols, few studies have allowed to fully determine microphysical proper-ties of volcanic sulfates in aged tropospheric plumes (e.g. Bukowiecki et al. (2011) in the upper-tropospheric Eyjafjallajökull cloud in 2010), due to the difficulty to isolate the signature of sulfate from co-existing meteorological clouds and/or aerosols of a different nature. Here, we use a wealth of complementary observations from in-situ ground-level sampling (SO_2 and

25   particulate matter), ground-based remote sensing (lidar, sun-photometry, UV-DOAS spectroscopy) available in Belgium and France, and satellite sensors (OMI and IASI) to characterize the distribution of volcanic SO_2 and sulfate aerosols as well as the dynamics of the planetary boundary layer (PBL). Both dynamical and microphysical properties of sulfate aerosols in the aged low-tropospheric Bárdarbunga cloud are provided.

We take advantage of this exceptional panel of observations to quantitatively examine and test our modeling ability to retrospectively reproduce the volcanogenic event of long-range air pollution taking place in late September 2014. While also relevant for industrial accident studies, such an exercise is critical to get prepared to accurately forecast a future large-scale episode of volcanogenic air pollution. Indeed, geological records indicate that Laki-style high-discharge lava flood eruptions, which emit huge amounts of sulphur compounds into the atmosphere, can occur in Iceland a few times per millennium (Thordarson and Larsen, 2007).

2 Methodology

2.1 Satellite/ground-based remote sensing and in-situ sampling

Given the low injection height of Bárdarbunga emissions (below 4 km), the Level-2 product of the ultraviolet-visible OMI/Aura satellite sensor for the SO_2 total column (NASA GES DISC, 2016) is mostly preferred to hyperspectral infrared IASI/Metop observations whose sensitivity decreases below 5 km. The center of mass of the SO_2 cloud is assumed to be within the PBL. North-south gaps in snapshots of the SO_2 cloud result from the so-called 'row anomaly' of OMI detector (www.knmi.nl/omi/research/product/rowanomaly-background) which alters radiance data at all wavelengths for particular viewing directions. In a complementary manner, IASI captures on 21 Sept the front of the SO_2 cloud which is largely missed by OMI due to the 'row anomaly'. The major advantage of IASI is that it can track the altitude of SO_2 (Clarisse et al., 2014), even from moderate eruptions (Boichu et al., 2015).

A continuously-operating ground-based platform, with various remote sensing instruments, is installed on the roof of the Laboratoire d'Optique Atmosphérique in Lille-Villeneuve d'Ascq (northern France). It includes a micro-pulse CIMEL lidar measuring the radiation elastically backscattered by atmospheric particles and molecules at 532 nm, which allows for determining the vertical distribution of aerosols as a function of time using the BASIC algorithm (Mortier et al., 2013). As illustrated in Fig. 1, meteorological clouds are clearly distinguished from low-tropospheric aerosols. The PBL is also detected by applying a wavelet covariance transform to lidar backscatter profiles averaged over 20 minutes (Brooks, 2003). The PBL top is defined as the location of the maximum in the covariance profiles. As low-level meteorological clouds may disturb PBL height retrieval, a filter is applied so as to provide only cloud-free heights.

[Figure 1 about here.]

Due to frequent cloudy conditions, time variations of vertically integrated aerosol properties derived from level-1.0 (not cloud-screened) and 2.0 (cloud-screened and quality assured) sunphotometric data from the AERONET network (Holben et al., 2001) are exploited using different inversion algorithms and combining two 80 km-distant sites (Lille and Dunkerque) (Fig. 2). Fine (sub-micron) and coarse (super-micron) aerosol optical depths (AOD) at 500 nm are retrieved using spectral deconvolution algorithm (SDA) applied on AOD within the range 340 to 1640 nm (O'Neill et al., 2003) (Fig. 2). Volume size distribution (VSD) of volcanic aerosols above Lille are determined using two different inversions: AERONET (version 2) standard algorithm which requires cloud-free almucantar observations (Dubovik and King, 2000; Dubovik et al., 2006) and

recently developed GRASP (Generalized Retrieval of Aerosol and Surface Properties) code (Dubovik et al., 2014). Over the period of study, there is only one almucantar in Lille fulfilling AERONET level-2.0 requirements (on 23 Sept). Therefore, for the other two days, VSD is retrieved using GRASP: on 21 Sept, GRASP inverts a (manually inspected) cloud-free principal plane as in AERONET almucantar standard inversion (Torres et al., 2014); on 22 Sept, direct sun (DS) measurements (available without information of sky radiances) are inverted. For this latter inversion of DS observations, we assume VSD to be a bi-modal lognormal function and optical properties (i.e. refractive index and sphericity parameter) identical to those retrieved from the almucantar on 23 Sept. The consistency of these algorithms and strategies is shown in Fig. 3. Using a multi-site approach (ie., including AERONET VSD determined in neighbouring site of Dunkerque, 80 km north west of Lille), the influence on the fine mode of cirrus co-existing with sulfate aerosol on 22 Sept in Lille is evidenced (Bottom of Fig. 3). SO_2 modeling in Fig. 7 shows that the volcanic cloud passes over Dunkerque a few hours before Lille. Therefore, the similarity of fine-mode components retrieved at Lille and Dunkerque indicates that cirrus in Lille weakly influence the fine-mode, which is in turn mainly associated with volcanic sulfate aerosols in this specific case.

[Figure 2 about here.]

[Figure 3 about here.]

Daily ground-based MAX(Multi-AXis)-DOAS observations in the ultraviolet are performed by BIRA-IASB in Brussels-Uccle (Belgium) and provide time series of SO_2 column amounts during daylight hours (time step of $\sim$ 12 min). The instrument is described in Gielen et al. (2014) while retrieval method and settings can be found in Wang et al. (2014).

Ground-level concentrations of SO_2 and particles are routinely measured in France by a network of ground stations managed by accredited associations responsible for air quality monitoring. For this study, AIRPARIF provided observations at Neuilly-sur-Seine (near Paris) and Atmo Nord–Pas-de-Calais at Calais and Lille-Fives (northern France). Ground-level SO_2 concentrations are monitored by ultraviolet fluorescence with a time step of 15 min. Mass concentration of particulate matter, with diameters less than 2.5 μm (PM2.5) and 10 μm (PM10), are measured by TEOM-FDMS (Tapered Element Oscillating Microbalances with Filter Dynamics Measurement Systems) (time step of 15 min) or by RST (Regulated Sampling Tube) beta gauge automated air monitors (time step of 2 hours) which account for both volatile and non-volatile PM fractions.

2.2 Chemistry-transport model

The atmospheric dispersion of volcanic SO_2 is described using the CHIMERE Eulerian regional chemistry-transport model (CTM) (Boichu et al., 2013, 2014, 2015). The model accounts for various physico-chemical processes affecting the SO_2 released in the atmosphere, including transport, turbulent mixing, diffusion, dry deposition, wet scavenging and gas-/aqueous-phase chemistry. However, the conversion of SO_2 to sulfate aerosols is not implemented in this study to avoid uncontrolled influence of uncertainties on the numerous factors governing this process in a volcanic cloud. CHIMERE CTM is driven by

meteorological fields from the Weather Research and Forecasting (WRF) model (Skamarock et al., 2008), which is forced by

15 NCEP (National Centers for Environmental Prediction) reanalysis data on a 6-h basis (Kalnay et al., 1996). WRF meteorological fields have a 25 km × 25 km horizontal grid and 30 hybrid sigma-pressure vertical layers extending up to ~ 19 km above sea level (a.s.l.). The dynamics of the PBL is described by the Yonsei University (YSU) scheme implemented in WRF (Hong et al., 2006). The calculated PBL height is then used as an input to CHIMERE. CHIMERE simulations are performed over the period 19–24 Sept 2014 on a large area extending from North of Greenland down to the south of France. CHIMERE CTM has

20 the same horizontal resolution as WRF but a finer vertical resolution with 29 hybrid sigma-pressure vertical layers extending up to 150 hPa (~ 13 km a.s.l.).

SO_2 emissions are poorly known. For simplicity, we model the source term as a step-function in time with an amplitude of 4700 t.h^{-1}, which roughly corresponds to peak values of the SO_2 flux retrieved from ground-based UV-DOAS spectroscopy (Gíslason et al., 2015). SO_2 is released along a Gaussian profile with a full width at half maximum of 100 m. Inception time

25 and altitude of emissions are found by trial and error so as to reproduce first-order features of satellite and ground-level SO_2 observations. We find that two step-functions at (1) 1 km a.s.l. from 19 Sept 2014 12:00 UT until 24 Sept 2014 00:00 UT and (2) at 4 km a.s.l. from 20 Sept 2014 12:00 UT until 24 Sept 2014 00:00 UT, are sufficient to fit the two-wave behaviour of the Bárdarbunga cloud (Fig. 5). This upper injection height is consistent with IASI level 2 products of SO_2 altitude, which captured the Bárdarbunga SO_2 cloud in the vicinity of the source on 19, 20, 22 and 23 Sept. 2014 (Fig. 4). Accordingly, this source term is not intended to reflect the full complexity of the actual emissions of Bárdarbunga but rather captures only the SO_2 parcels traveling toward Western Europe.

[Figure 4 about here.]

5 ## 3   Results

3.1   Large-scale SO_2 dispersal from Iceland toward Europe

According to OMI satellite observations, the model reproduces the correct timing of SO_2 arrival in northern Scotland on 20 Sept 2014 descending down to the south-western coast of England on 21 Sept (Fig. 5). SO_2 observed to the north of 60°N and to the east of 5°W on 21 Sept is absent from simulations because emissions prior to 19 Sept are not accounted for as they

10 remain at high latitude, outside the domain of interest. The model indicates a first SO_2 wave (wave 1 in Fig. 5) hitting Belgium and northern France on 21 Sept, which cannot be confirmed by OMI observations, hampered above France due to north-south gaps resulting from detector 'row-anomaly'. It is however captured by IASI (inset in Top of Fig. 5). This first wave is then pushed and dispersed toward the Atlantic Ocean. On 22 Sept, both model and observations depict a north-south elongated SO_2 cloud hitting France for the second time (wave 2). Modeled SO_2 column amounts are in agreement with OMI SO_2 loading.

15 However, the absence of SO_2 above Fenno-Scandinavia in the OMI image contradicts the model. This inconsistency may result from inaccuracies of prescribed altitudes of SO_2 injection or of meteorological forcing of the model. On 23 Sept, the model shows the arrival of SO_2 above Norway/Sweden, after a long transport from Iceland up to northern Greenland. On the same

day, model and observations both indicate some dispersed remnants (although of different intensity) of the second SO_2 wave having hit western Europe above western France and southern UK.

20   [Figure 5 about here.]

3.2 Arrival of the volcanic cloud in the far-range lower troposphere

The precise timing of arrival of the Bárdarbunga cloud in the French lower troposphere on 21 Sept 2014 is deduced from the synergetic analysis of volcanic SO_2 modeling as well as observations from ground-based lidar and sunphotometers which remotely sense aerosols, on a continuous basis, above Lille-Villeneuve d'Ascq. Sunphotometry indicates the arrival of fine

25 mode aerosols between 12:00 and 15:30 UT on 21 Sept (Fig. 6-a1), presumably sulfate aerosols formed from volcanic SO_2 in the atmosphere, according to their high single scattering albedo (~ 0.98) derived from AERONET inversions indicative of non- or weakly-absorbing aerosols. While fine mode AOD values remain below 0.1 at midday in Lille on 21 Sept, the arrival of volcanic sulfate aerosols marks an increase in AOD with values ranging between 0.3 and 0.45 in the afternoon (Fig. 2). Principal plane inversion also provides volume size distribution (Fig. Fig. 6-a2), with an effective radius (r_{eff}) of these sulfate of 0.21 μm (mean volume radius r_v of 0.26 μm). Simultaneously, lidar active observations, which characterize the temporal evolution of aerosol vertical distribution, indicate the presence above Lille of aerosols at 2 km a.s.l., with a decreasing altitude with time (Fig. 6-b). This behavior of aerosols coincides with the temporal decrease of the modeled altitude of the most concentrated

5 layer of volcanic SO_2 accompanying the first SO_2 wave described in Section 3.1 (red line in Fig. 6-b). This common evolution evidences the co-existence of SO_2 and sulfate aerosols within the low-altitude volcanic cloud. Soon thereafter, ground-level sampling in Lille records the first significant increase of SO_2 concentration up to ~ 20 μg.m^{-3} (compared to background values usually close to zero at this site except when contaminated by nearby urban heating plant) followed by a first rise in particulate matter abundance up to ~ 35 μg.m^{-3} (Fig. 6-c). Hence, these four pieces of evidence (SO_2 modeling, sunphotometry, lidar

10 and ground-level air sampling) unambiguously confirm the arrival of the Bárdarbunga cloud in the French lower troposphere down to the ground in the early afternoon of 21 Sept.

After a period of quiescence, a second, more prolonged and intense episode of ground-level air pollution, in both SO_2 and particles, is recorded from 22 to 23 Sept in Lille (Fig. 6-c). During this second episode, the PM concentration exceeds the information and recommendation threshold prescribed by WHO of ~ 50 μg.m^{-3}, defined as the hourly running 24 hour

15 average value. Concomitantly, sunphotometry indicates a persistent fine-mode (Fig. 6-a2) of weakly absorbing aerosols, which produce fine mode AOD values abnormally high for Lille and nearby Dunkerque (up to ~ 0.8, Fig. 2). The size of Bárdarbunga sulfate aerosols (r_{eff} within 0.26–0.28 μm, r_v within 0.21–0.24 μm) largely exceeds the radius characterizing typical urban aerosols in Lille ($r_{eff} < 0.2$ μm (Mortier, 2013)). This size is also larger than values reported by sparse observations of volcanic tropospheric sulfate radius at distance from the volcanic source (r_v within 0.12–0.16 μm in the Eyjafjallajökull cloud

20 (Bukowiecki et al., 2011)).

                                    [Figure 6 about here.]

3.3 Far-range air pollution at ground level

Substantial increases in ground-level SO_2 concentration are recorded by air quality monitoring networks not only in the north end of the country but also on a broad regional scale in France. Unseen for more than a decade, this makes this event of SO_2 pollution exceptional (Fig. 7). Interestingly, this pollution episode strictly follows a similar temporal pattern, except for a time lag, whichever the city of observation. As observed from space and reproduced by CTM simulations at a large scale (Section 3.1), two main waves of SO_2 hit France from 21 to 23 Sept. At ground-level, air quality measurements track the progressive transport of these two waves from the north to the center of France (blue lines in Fig. 7). SO_2 concentrations up to 70 $\mu g.m^{-3}$ are associated with the second wave, which is recorded firstly in Calais, then successively 3 hours later in Lille-Fives and 8 hours later much further south near Paris in Neuilly-sur-Seine. While the modelled time series of SO_2 column amounts reproduce this two-wave pattern (solid red line in Fig. 7), simulations fail in correctly describing ground-level SO_2 concentration as the second wave of pollution starting on 22 Sept is missed (dashed red line in Fig. 7).

[Figure 7 about here.]

4 Discussion: how to improve long-distance air quality modeling?

As illustrated by the broad agreement with OMI satellite data (Fig. 5 and Section 3.1), the chemistry-transport model is efficient at reproducing on a continental scale the dispersion of the Bárdarbunga SO_2 cloud from Iceland toward France. The temporal dynamics of far-range events of air pollution, characterized for instance in France by the arrival of two distinct SO_2 waves traveling from north toward the capital city in $\sim$ 8 hours, is hence well described (solid red line in Fig. 7). A good agreement is also reached between model and observations of SO_2 vertical column amounts (CA) by ground-based UV max-DOAS spectroscopy performed at long distance from the eruptive site in Uccle/Belgium, located less than 100 km from Lille/France (Fig. 8). Model and observations find SO_2 CA of the same magnitude on 19, 20, 22 and 23 Sept. Nevertheless, the model cannot capture the significant and abrupt SO_2 CA increase (up to 14 DU) of very short duration (from 14:18 to 15:07 UT) observed on 21 Sept by DOAS, likely due to the insufficient (hourly) time resolution of the model.

[Figure 8 about here.]

However, the model has difficulty reproducing the correct intensity of the air pollution episode in remote areas and it misses the second wave of SO_2 at ground-level in the north of France (dashed red line in Fig. 7). This shortcoming results from an incorrect description of the vertical distribution of SO_2 at long distance from the eruptive site. According to lidar observations capable to detect sulfate aerosols coexisting with SO_2 (Section 3.2), the model mimics correctly the drop in altitude above Lille of the first SO_2 wave on 21 Sept (red line in Fig. 6-b). This modeled wave hits the surface at about the same time as the first detection of air pollution at ground-level. But the second modeled wave, despite a similar pattern with a significant decrease in altitude with time from 6 km a.s.l., does not reach the ground and remains at an altitude $\geq$ 1.8 km above Lille on 22 Sept (red line in Fig. 6-b).

This discrepancy can result from a limited knowledge of SO_2 emission parameters (flux and altitude of injection) which initialize the chemistry-transport model. As is commonly the case for newly erupting volcanoes, only sparse ground-based observations of SO_2 flux and injection height were available during the Bárdarbunga eruption (Gíslason et al., 2015). Inverse modeling, which combines satellite observations of volcanic SO_2 with a chemistry-transport model, can fulfill this need as it allows for characterizing SO_2 emission flux and injection height at a high temporal resolution during an eruptive crisis

5 (Eckhardt et al., 2008; Boichu et al., 2013; Theys et al., 2013; Flemming and Inness, 2013; Moxnes et al., 2014; Boichu et al., 2015). In addition to the impact on vertical transport of advection schemes in Eulerian CTM (Freitas et al., 2012), refined emission parameters should improve the quality of modeled horizontal but also vertical distribution of volcanic SO_2 in the far-range.

Issues encountered for adequately modeling long-distance air pollution episodes also arise from the difficulty to correctly

10 model the capture and mixing of volcanic SO_2 in the far-range PBL. The altitude of the PBL above Lille is retrieved from lidar observations and compared with model output in Fig. 9. Simulations generally underestimate the PBL height (up to 1.5 km), especially in the mornings and evenings. This is a relatively well-known limitation of WRF PBL schemes (Banks et al., 2015), which are used here to force the CHIMERE CT model. In a context of urban air pollution, where pollutants are injected at ground-level into the atmosphere, underestimation of the PBL height favors an over-evaluation of the intensity of ground-level

15 pollution. In our volcanic case-study, this may explain the overestimation of the SO_2 ground concentration increase resulting from the first SO_2 wave reaching the ground of Lille on 21 Sept in the evening (red dashed line in Top of Fig. 7). However, the PBL height underestimation by the model can also prevent from correctly capturing the second SO_2 wave in the PBL, as it travels at a higher altitude (red line in Fig. 6-b). In this context, the intensity of air pollution at ground-level is under-evaluated, if not missed. A better description of surface air pollution episodes in remote areas may necessitate a higher spatial resolution

20 of both CTM and WRF models (Colette et al., 2014). However, the study of far-range volcanogenic air pollution events at high temporal resolution (hourly here) demands an accurate modeling of both the long-range transport of volcanic compounds and the meteorological dynamics at a local scale. Therefore, a higher spatial resolution would imply both high computation time and capacity. This requirement seriously challenges our current modeling capacities. Further explorations are needed to find optimum configuration settings which would be acceptable not only for retrospective analysis but also for the forecast of

25 far-range air pollution episodes triggered by future eruptions releasing large amounts of toxic gases to the atmosphere.

[Figure 9 about here.]

5 Conclusions

The Bárdarbunga eruption provides the exceptional opportunity to carry out a modelling exercise of a far-range volcanogenic air pollution event using a broad panel of complementary measurements acquired by space and ground-based (remote sensing and in-situ) sensors.

Chemistry-transport modeling reproduces the large-scale dispersal of SO_2 from Iceland toward western Europe as observed

5 from satellite OMI and IASI sensors. The synergetic analysis of SO_2 modeling and aerosol dynamics deduced from sunpho-

tometric and lidar observations allows us to determine the exact timing of arrival of the volcanic cloud in the distant lower troposphere of northern France before its descent to the ground. The joint analysis of lidar measurements with the retrieval of multi-site sunphotometric observations using recently-developed inversion algorithms also provides a full characterization of volcanic sulfate aerosol properties with time (loading, vertical repartition, size distribution and single scattering albedo).

10   Based on this combined analysis of volcanic SO_2 and sulfate aerosols, we highlight the success and the challenges in simulating far-range episodes of air pollution. The temporal dynamics of the air pollution event is well described, but the model faces difficulties in reproducing the correct magnitude of the SO_2 concentration at ground-level. Among several identified sources of limitations, analysis of lidar observations points out the difficulties to accurately simulate the boundary layer dynamics in remote areas. Such barriers will need to be overcome in order to get prepared to accurately forecast future large-scale

15   volcanogenic events of air pollution.

Acknowledgements. M. Boichu gratefully acknowledges support from the Nord–Pas-De-Calais Regional Council for her junior research fellowship. LOA members thank the French National Research Agency for funding the VOLCPLUME project (ANR-15-CE04-0003-01), the Chantier Arctique for funding the PARCS project and the CaPPA (Chemical and Physical Properties of the Atmosphere) excellence laboratory. NASA Goddard Earth Sciences Data and Information Services Center (GES DISC) are acknowledged for providing OMI SO_2

20   data. BIRA-IASB MAX-DOAS activities at Uccle were financially supported by the projects AGACC-II (BELSPO, Brussels) and NORS (EU FP7; contract 284421). S.B. and L.C are respectively Research Fellow and Research Associate with the Belgian F.R.S-FNRS. Researchers and agencies in charge of AERONET (sunphotometry) and air quality monitoring networks (Atmo NPDC and AIRPARIF) provided invaluable observations and are gratefully thanked. Authors warmly thank Y. Derimian (LOA) for discussions on the impact of cirrus on sunphotometric retrievals.

25 References

Ayris, P. M. and Delmelle, P.: The immediate environmental effects of tephra emission, Bull. Volcanol., 74, 1905–1936, 2012.

Banks, R. F., Tiana-Alsina, J., Rocadenbosch, F., and Baldasano, J. M.: Performance evaluation of the boundary-layer height from lidar and the Weather Research and Forecasting model at an urban coastal site in the north-east Iberian Peninsula, Boundary-Layer Meteorology, 157, 265–292, 2015.

Boichu, M.: Pollution de l'air en France: le volcan Bárdarbunga en cause, La Météorologie, 89, 4 – 6, doi:10.4267/2042/56589, http://hdl.handle.net/2042/56589, 2015.

Boichu, M., Menut, L., Khvorostyanov, D., Clarisse, L., Clerbaux, C., Turquety, S., and Coheur, P.-F.: Inverting for volcanic SO_2 flux at high temporal resolution using spaceborne plume imagery and chemistry-transport modelling: the 2010 Eyjafjallajökull eruption case study, Atmos. Chem. Phys., 13, 8569–8584, doi:10.5194/acp-13-8569-2013, 2013.

Boichu, M., Clarisse, L., Khvorostyanov, D., and Clerbaux, C.: Improving volcanic sulfur dioxide cloud dispersal forecasts by progressive assimilation of satellite observations, Geophys. Res. Lett., 41, 2637–2643, doi:10.1002/2014GL059496, 2014.

Boichu, M., M., Clarisse, L., Péré, J.-C., Herbin, H., Goloub, P., Thieuleux, F., Ducos, F., Clerbaux, C., and Tanré, D.: Temporal variations of flux and altitude of sulfur dioxide emissions during volcanic eruptions: implications for long-range dispersal of volcanic clouds, Atmos. Chem. Phys., 15, 8381–8400, 2015.

Brooks, I. M.: Finding boundary layer top: Application of a wavelet covariance transform to lidar backscatter profiles, Journal of Atmospheric and Oceanic Technology, 20, 1092–1105, 2003.

Bukowiecki, N., Zieger, P., Weingartner, E., Jurányi, Z., Gysel, M., Neininger, B., Schneider, B., Hueglin, C., Ulrich, A., Wichser, A., et al.: Ground-based and airborne in-situ measurements of the Eyjafjallajökull volcanic aerosol plume in Switzerland in spring 2010, Atmos. Chem. Phys., 11, 10 011–10 030, 2011.

Clarisse, L., Coheur, P.-F., Theys, N., Hurtmans, D., and Clerbaux, C.: The 2011 Nabro eruption, a SO_2 plume height analysis using IASI measurements, Atmos. Chem. Phys., 14, 3095–3111, 2014.

Colette, A., Bessagnet, B., Meleux, F., Terrenoire, E., and Rouil, L.: Frontiers in air quality modelling, Geoscientific Model Development, 7, 203–210, 2014.

Delmelle, P.: Environmental impacts of tropospheric volcanic gas plumes, Geological Society, London, Special Publications, 213, 381–400, 2003.

Dubovik, O. and King, M. D.: A flexible inversion algorithm for retrieval of aerosol optical properties from Sun and sky radiance measurements, J. Geophys. Res. Atm., 105, 20 673–20 696, 2000.

Dubovik, O., Sinyuk, A., Lapyonok, T., Holben, B. N., Mishchenko, M., Yang, P., Eck, T. F., Volten, H., Munoz, O., Veihelmann, B., et al.: Application of spheroid models to account for aerosol particle nonsphericity in remote sensing of desert dust, J. Geophys. Res. Atm., 111, 2006.

Dubovik, O., Lapyonok, T., Litvinov, P., Herman, M., Fuertes, D., Ducos, F., Lopatin, A., Chaikovsky, A., Torres, B., Derimian, Y., et al.: GRASP: a versatile algorithm for characterizing the atmosphere, SPIE Newsroom, 2014.

Eckhardt, S., Prata, A. J., Seibert, P., Stebel, K., and Stohl, A.: Estimation of the vertical profile of sulfur dioxide injection into the atmosphere by a volcanic eruption using satellite column measurements and inverse transport modeling, Atmos. Chem. Phys., 8, 3881–3897, 2008.

5   European Environment Agency, .: Sulphur dioxide (SO$_2$) emissions, "http://www.eea.europa.eu/data-and-maps/
    indicators/eea-32-sulphur-dioxide-so2-emissions-1/assessment-3", http://www.eea.europa.eu/data-and-maps/indicators/
    eea-32-sulphur-dioxide-so2-emissions-1/assessment-3, "[Online; accessed 22-Dec-2015]", 2014.

    Flemming, J. and Inness, A.: Volcanic sulfur dioxide plume forecasts based on UV satellite retrievals for the 2011 Grimsvötn and the 2010
    Eyjafjallajökull eruptions, J. Geophys. Res., doi:10.1002/jgrd.50753, 2013.

10 Freitas, S., Rodrigues, L. F., Longo, K. M., and Panetta, J.: Impact of a monotonic advection scheme with low numerical diffusion on
    transport modeling of emissions from biomass burning, J. Adv. Model. Earth Syst., 4, 2012.

    Gielen, C., Van Roozendael, M., Hendrick, F., Pinardi, G., Vlemmix, T., De Bock, V., De Backer, H., Fayt, C., Hermans, C., Gillotay, D.,
    and Wang, P.: A simple and versatile cloud-screening method for MAX-DOAS retrievals, Atmosph. Meas. Techn., 7, 3509–3527, 2014.

    Gíslason, S., Stefánsdóttir, G., Pfeffer, M., Barsotti, S., Jóhannsson, T., Galeczka, I., Bali, E., Sigmarsson, O., Stefánsson, A., Keller, N.,
15 et al.: Environmental pressure from the 2014–15 eruption of Bárdarbunga volcano, Iceland, Geochem. Perspect. Lett, 1, 84–93, 2015.

    Grahn, H., von Schoenberg, P., and Brännström, N.: What's that smell? Hydrogen sulphide transport from Bardarbunga to Scandinavia, J.
    Volcanol. Geoth. Res., 303, 187–192, 2015.

    Grattan, J., Rabartin, R., Self, S., and Thordarson, T.: Volcanic air pollution and mortality in France 1783–1784, Comptes Rendus Geoscience,
    337, 641–651, 2005.

20 Hansell, A. and Oppenheimer, C.: Health hazards from volcanic gases: a systematic literature review, Archives of Environmental Health: An
    International Journal, 59, 628–639, 2004.

    Holben, B., Smirnov, A., Eck, T., Slutsker, I., Abuhassan, N., Newcomb, W., Schafer, J., Tanre, D., Chatenet, B., and Lavenu, F.: An emerging
    ground-based aerosol climatology- Aerosol optical depth from AERONET, J. Geophys. Res., 106, 12 067–12 097, 2001.

    Hong, S.-Y., Noh, Y., and Dudhia, J.: A new vertical diffusion package with an explicit treatment of entrainment processes, Monthly Weather
25 Review, 134, 2318–2341, 2006.

    Horwell, C. J. and Baxter, P. J.: The respiratory health hazards of volcanic ash: a review for volcanic risk mitigation, Bull. Volcanol., 69,
    1–24, 2006.

    Ialongo, I., Hakkarainen, J., Kivi, R., Anttila, P., Krotkov, N., Yang, K., Li, C., Tukiainen, S., Hassinen, S., and Tamminen, J.: Validation
    of satellite SO$_2$ observations in northern Finland during the Icelandic Holuhraun fissure eruption, Atmos. Meas. Techn., 8, 2279–2289,
    doi:10.5194/amt-8-2279-2015, 2015.

5   Kalnay, E., Kanamitsu, M., Kistler, R., Collins, W., Deaven, D., Gandin, L., Iredell, M., Saha, S., White, G., Woollen, J., et al.: The
    NCEP/NCAR 40-year reanalysis project, Bull. Am. Meteo. Soc., 77, 437–471, 1996.

    Longo, B., Rossignol, A., and Green, J.: Cardiorespiratory health effects associated with sulphurous volcanic air pollution, Public health,
    122, 809–820, 2008.

    Mortier, A.: Tendances et variabilités de l'aérosol atmosphérique à l'aide du couplage Lidar/Photomètre sur les sites de Lille et Dakar, Ph.D.
10 thesis, Lille 1, 2013.

    Mortier, A., Goloub, P., Podvin, T., Deroo, C., Chaikovsky, A., Ajtai, N., Blarel, L., Tanre, D., and Derimian, Y.: Detection and characteriza-
    tion of volcanic ash plumes over Lille during the Eyjafjallajökull eruption, Atmos. Chem. Phys., 13, 3705–3720, 2013.

    Moxnes, E., Kristiansen, N., Stohl, A., Clarisse, L., Durant, A., Weber, K., and Vogel, A.: Separation of ash and sulfur dioxide during the
    2011 Grímsvötn eruption, J. Geophys. Res., 2014.

15 NASA GES DISC, .: OMI SO2 product, "http://disc.sci.gsfc.nasa.gov/Aura/data-holdings/OMI/omso2_v003.shtml", http://disc.sci.gsfc.
    nasa.gov/Aura/data-holdings/OMI/omso2_v003.shtml, 2016.

O'Neill, N., Eck, T., Smirnov, A., Holben, B., and Thulasiraman, S.: Spectral discrimination of coarse and fine mode optical depth, J. Geophys. Res. Atmos., 108, 2003.

Oppenheimer, C.: Eruptions that shook the world, Cambridge University Press, 2011.

20 Schmidt, A., Ostro, B., Carslaw, K. S., Wilson, M., Thordarson, T., Mann, G. W., and Simmons, A. J.: Excess mortality in Europe following a future Laki-style Icelandic eruption, Proceedings of the National Academy of Sciences, 108, 15 710–15 715, 2011.

Schmidt, A., Leadbetter, S., Theys, N., Carboni, E., Witham, C. S., Stevenson, J. A., Birch, C. E., Thordarson, T., Turnock, S., Barsotti, S., et al.: Satellite detection, long-range transport, and air quality impacts of volcanic sulfur dioxide from the 2014–2015 flood lava eruption at Bárdarbunga (Iceland), J. Geophys. Res. Atm., 120, 9739–9757, 2015.

25 Skamarock, J., Klemp, W., Dudhia, J., Gill, D., Barker, D., Duda, M., Huang, X., Wang, W., and Powers, J.: A description of the advanced research WRF version 3, NCAR technical note, NCAR/TN–475+ STR, 2008.

Theys, N., Campion, R., Clarisse, L., Brenot, H., Van Gent, J., Dils, B., Corradini, S., Merucci, L., Coheur, P.-F., Van Roozendael, M., et al.: Volcanic SO_2 fluxes derived from satellite data: a survey using OMI, GOME-2, IASI and MODIS, Atmos. Chem. Phys., 13, 5945–5968, doi:10.5194/acp-13-5945-2013, 2013.

Thordarson, T. and Larsen, G.: Volcanism in Iceland in historical time: volcano types, eruption styles and eruptive history, J. Geodyn., 43, 118–152, 2007.

Thordarson, T. and Self, S.: Atmospheric and environmental effects of the 1783-1784 Laki eruption: A review and reassessment, J. Geophys.
5 Res., 108, 4011, doi:10.1029/2001JD002042, 2003.

Torres, B., Dubovik, O., Toledano, C., Berjon, A., Cachorro, V., Lapyonok, T., Litvinov, P., and Goloub, P.: Sensitivity of aerosol retrieval to geometrical configuration of ground-based sun/sky radiometer observations, Atmos. Chem. Phys., 14, 847–875, 2014.

van Manen, S. M.: Perception of a chronic volcanic hazard: persistent degassing at Masaya volcano, Nicaragua, J. Appl. Volcanol., 3, 1–16, 2014.

10 Wang, T., Hendrick, F., Wang, P., Tang, G., Clémer, K., Yu, H., Fayt, C., Hermans, C., Gielen, C., Müller, J.-F., Pinardi, G., Theys, N., Brenot, H., and Van Roozendael, M.: Evaluation of tropospheric SO_2 retrieved from MAX-DOAS measurements in Xianghe, China, Atm. Chem. Phys., 14, 11 149–11 164, 2014.

Witham, C. S. and Oppenheimer, C.: Mortality in England during the 1783–84 Laki Craters eruption, Bull. Volcanol., 67, 15–26, 2004.

Yiou, P., Boichu, M., Vautard, R., Vrac, M., Jourdain, S., Garnier, E., Fluteau, F., and Menut, L.: Ensemble meteorological reconstruction
15 using circulation analogues of 1781–1785, Climate of the Past, 10, 797–809, doi:10.5194/cp-10-797-2014, 2014.
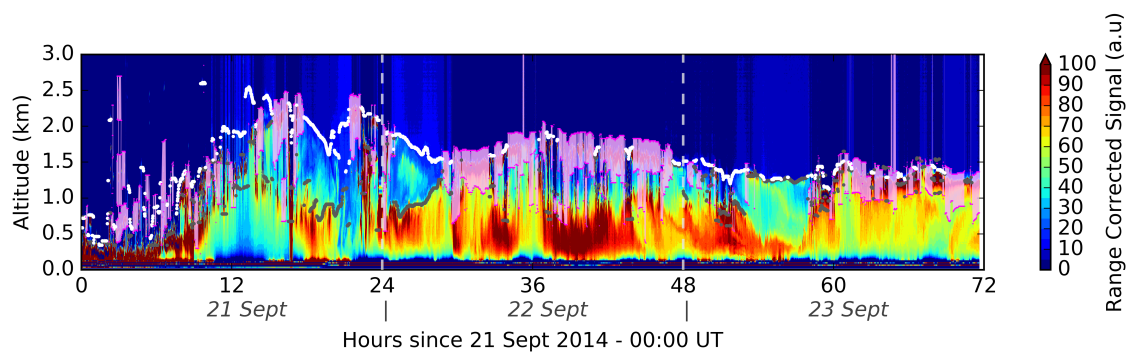
Figure 1. Detection of meteorological clouds above 300 m a.s.l. (pink), top of the aerosol layer (white) and top of the planetary boundary layer (grey) using BASIC algorithm from 21 to 23 Sept 2014 in Lille.
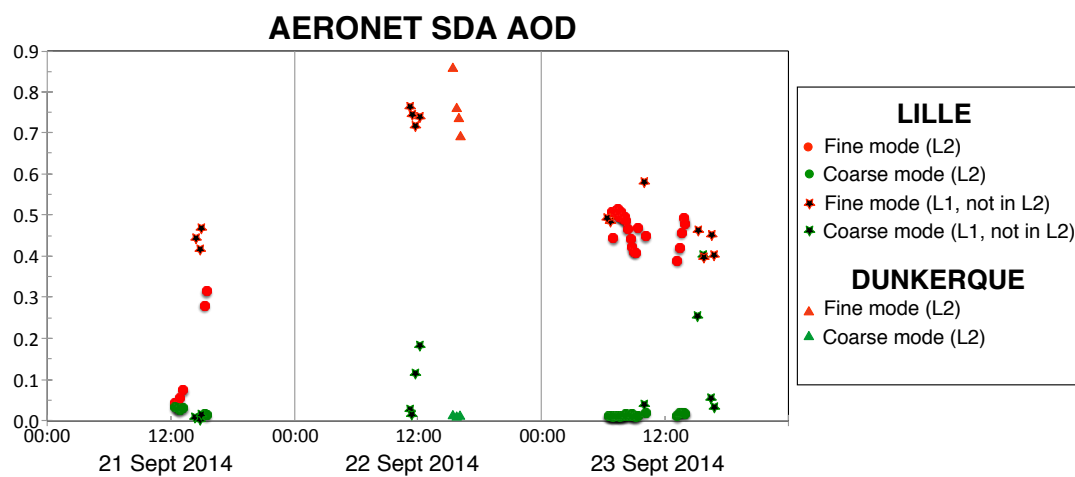
Figure 2. AERONET sunphotometric fine and coarse mode aerosol optical depth (AOD) at 500 nm retrieved using SDA algorithm in Lille and Dunkerque (located near Calais, 80 km north-west of Lille) from 21 Sept to 23 Sept 2014.
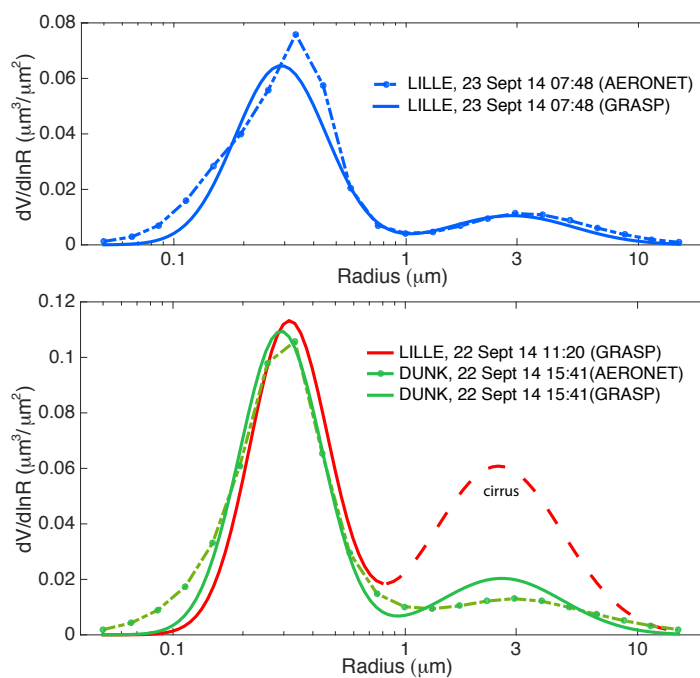
Figure 3. (Top) Consistency of the volume size distribution (VSD) in Lille on 23 Sept retrieved (dashed line) by inversion of Almucantar observations using standard AERONET inversion and (solid line) by inversion of direct sun measurements using GRASP algorithm. (Bottom) For 22 Sept, consistency of VSD retrieved by inversion of almucantar using standard AERONET inversion in Dunkerque (green dashed line) and by inversion of direct sun measurements using GRASP algorithm in Dunkerque (green plain line) and Lille (red line).
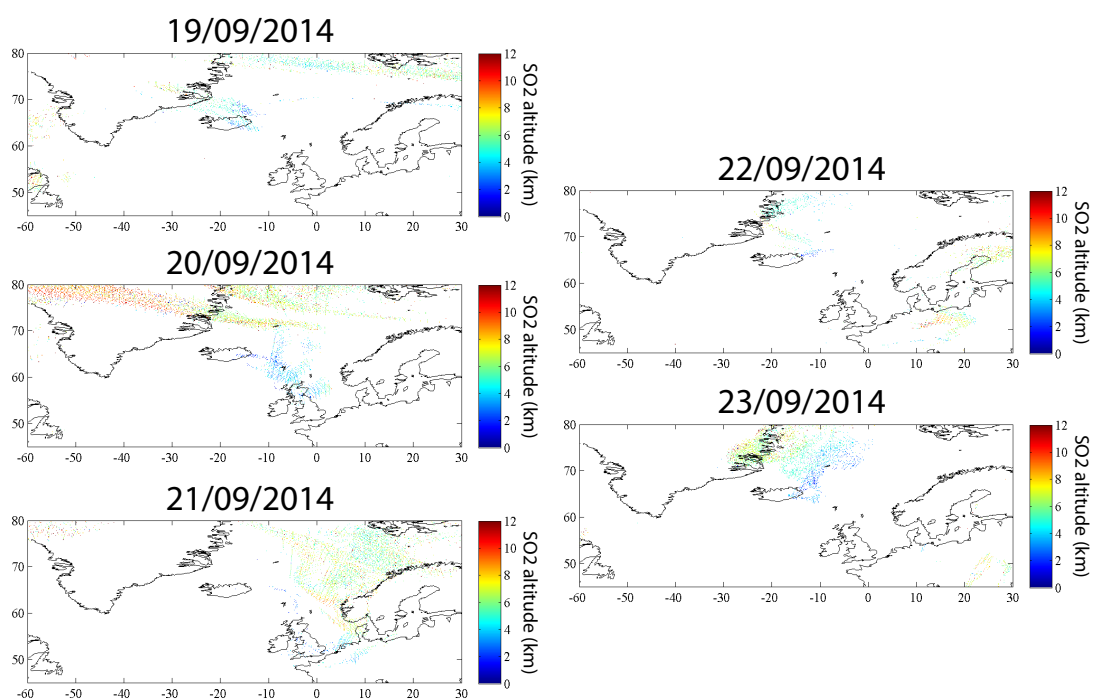
Figure 4. Altitude (in km a.s.l.) of Bárdarbunga SO$_2$ retrieved from IASI observations.
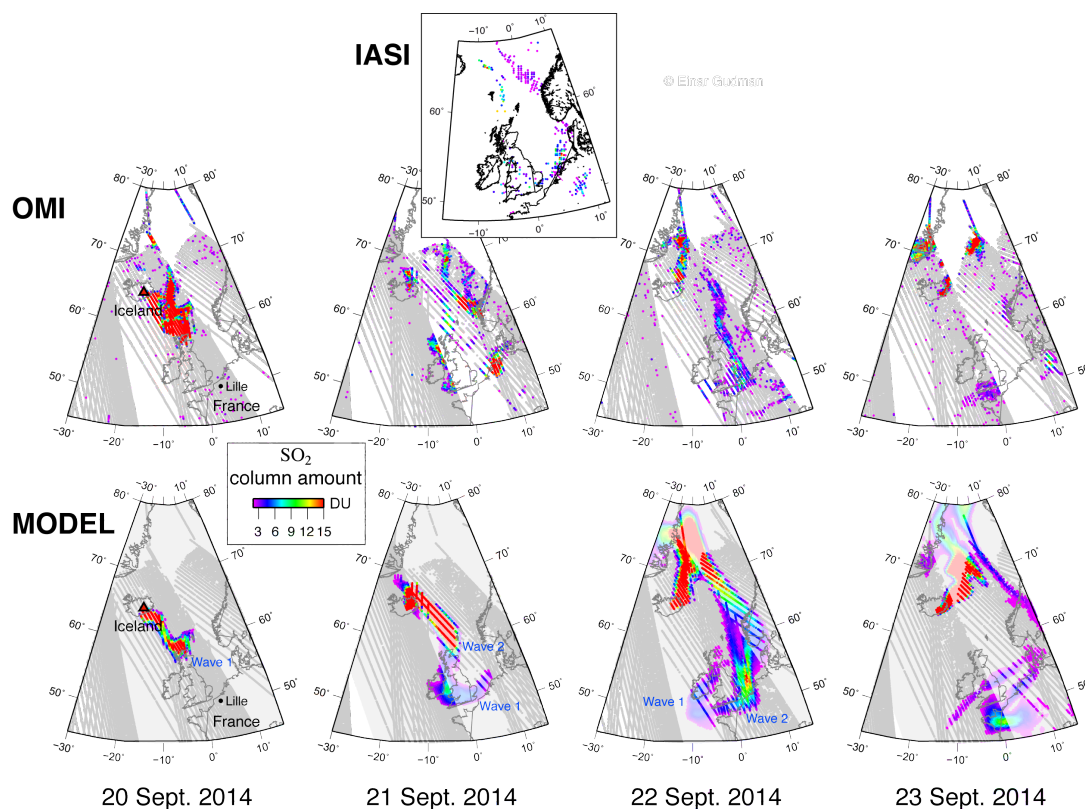
Figure 5. Dispersion of SO_2 from Bárdarbunga eruption toward Europe in late September 2014 (top) observed from satellite imagery (timeseries of OMI PBL products and IASI data in inset for 21 Sept) and (bottom) modeled using CHIMERE chemistry-transport model. Grey points indicate OMI column amounts < 2 DU. White zones show areas where data are not available. To facilitate the comparison between model and observations, the model is displayed transparently over zones where OMI data are not available.
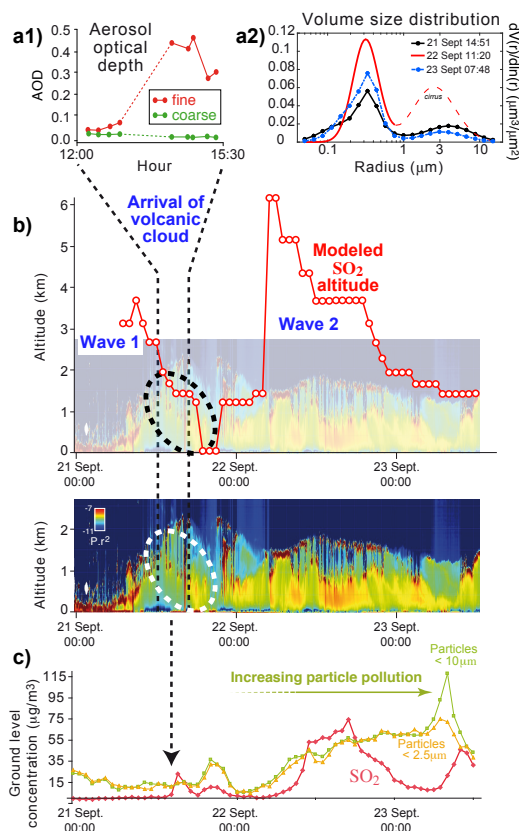
Figure 6. Multi-parametric observations and modeling of SO_2 and aerosols in Lille: (a) Retrieval of sunphotometric observations yields (a1) aerosol optical depth (at 500 nm) for coarse (green) and fine (red) mode on 21 Sept and (a2) time variations of aerosol volume size distribution. (b) Time series of the modeled altitude (red line) of the most concentrated layer of volcanic SO_2 overlaid on the lidar range-corrected backscatter signal ($\ln(P.r^2)$) at 532 nm. Distinction between aerosol and meteorological clouds in lidar data is shown in Fig. 1. (c) Ground-level concentration of SO_2 (red) and particles (PM2.5 in yellow and PM10 in green).
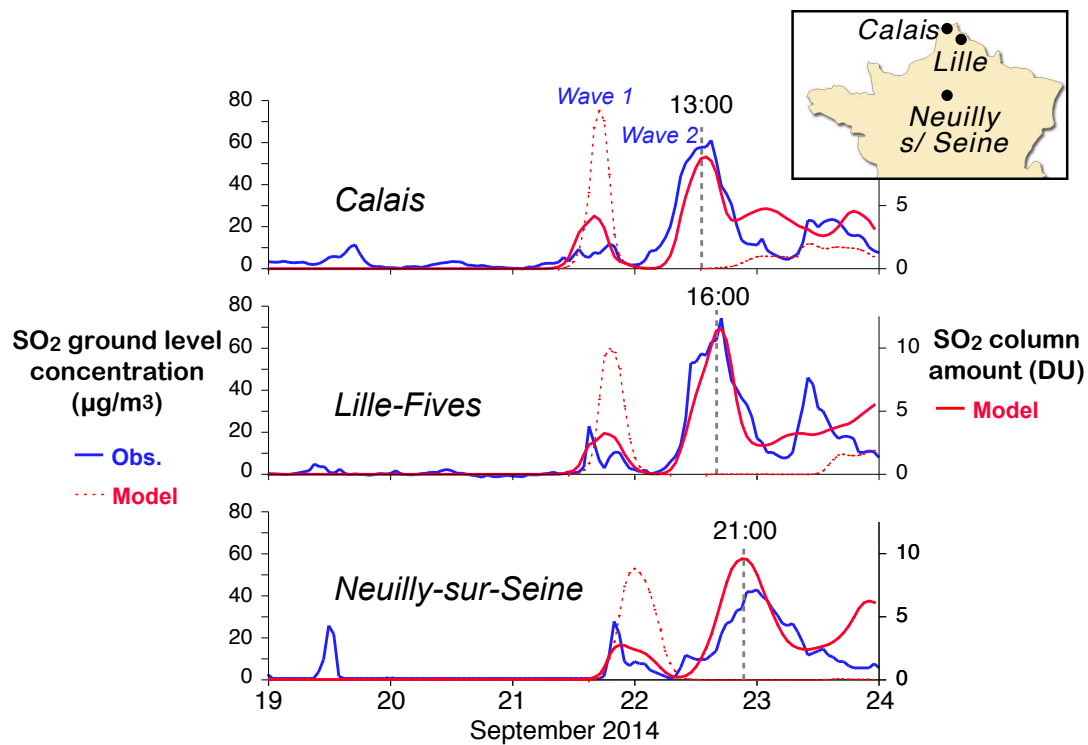
Figure 7. SO$_2$ ground-level concentration observed by air quality networks in France (blue) and modelled (dotted red), compared with modelled SO$_2$ vertical column amount (solid red).
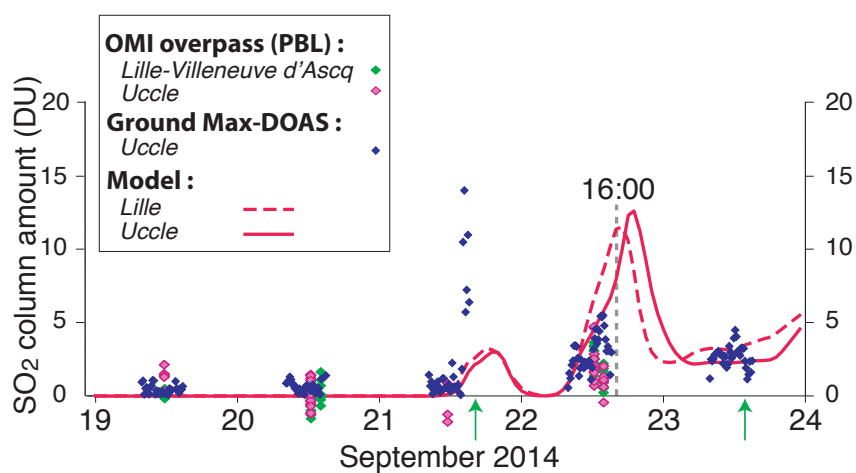
Figure 8. Time series of SO₂ vertical column amount above Uccle (Belgium) and Lille (France) from CHIMERE CT model (dashed and solid red lines for Lille and Uccle resp.), OMI PBL overpass (green and pink diamonds for Lille and Uccle resp.) and ground-based UV MAX-DOAS observations in Uccle (blue diamonds). Green arrows indicate when OMI overpasses above Lille are missing due to gaps in data related to sensor 'row anomaly'.
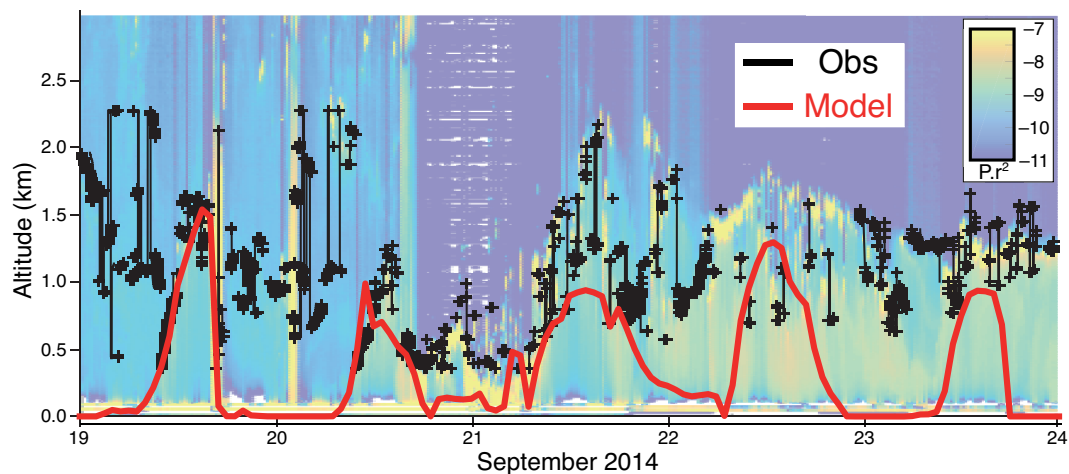
Figure 9. Height of the planetary boundary layer over Lille (red) calculated using CHIMERE CTM forced by WRF meteorological fields and (black) retrieved from lidar observations (range-corrected backscatter signal at 532 nm in background).